Electronic Supplementary Information (ESI) for

Theoretical study of the tuning role of β-methylthio or β-methylselenyl on charge transport properties of acenedithiophenes derivatives

Hui-yuan Li[a], Gui-ya Qin[a], Pan-pan Lin[c], Xiao-qi Sun[b], Jian-xun Fan[d], Rui Wang[a], Hui Li[a], Lu-yi Zou[a], Jing-fu Guo[b], Ai-min Ren[a]*

a Laboratory of Theoretical and Computational Chemistry, Institute of Theoretical Chemistry, College of Chemistry, Jilin University, Changchun, 130023, P.R. China.

*E-mail: aimin_ren@yahoo.com ; renam@jlu.edu.cn

b School of Physics, Northeast Normal University, Changchun 130024, P.R. China.

c College of Chemistry and Chemistry Engineering, Qiqihar University, Qiqihar, 161006, P.R. China.

d College of Chemistry and Materials Science, Weinan Normal University, Weinan 714000, China.

Table of Contents

Results and Discussion

S1. Carrier injection capability and stability

Overall, the HOMO values of anti-β-MT-XDT and anti-β-MS-XDT are all in the range of -5.03~-5.44 eV, compared with the Au that owns 5.10 eV work function,[1] which is exactly the injection barrier easy for hole transmission. In contrast, the LUMO value are in -1.47~-2.37 eV, which will lead to a high electron injection barrier that is not conducive to electron injection. In addition, the stability of material molecules in the environment is another problem that needs to be carefully

considered. Hence, IP and EA are introduced to represent the reduction and oxidation capabilities respectively, which can be used to evaluate the oxidation stability of materials, which are calculated at the B3LYP/6-311+G(d,p) level and shown in **Table 1**. In order to protect n-type transport materials from the invasion of free radical anions in the atmospheric environment, their EA value should reach 2.80 eV. [2] From **Table 1**, the EA values of the molecules studied in our system are all in the range of 0.42~1.22 eV, far lower than the value required, obviously are not suitable for n-type materials. On contrary, the IP value is 6.20~6.79 eV, which is so lower ionization potential that making it have better oxidation resistance as a p-type material molecule. Therefore, the molecules studied in this paper are potential p-type transport materials, which is consistent with the experimental results.

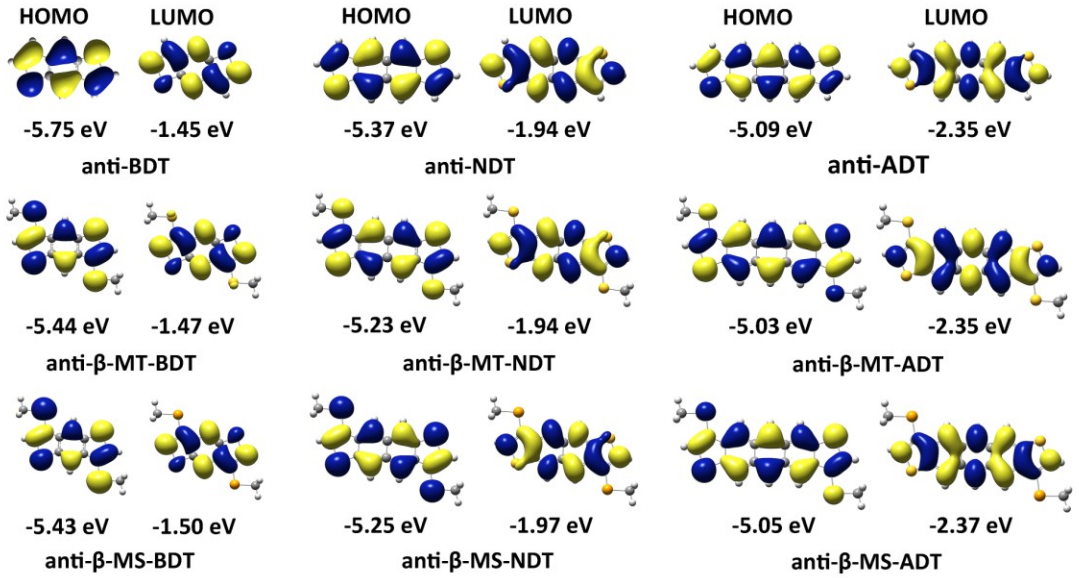

Fig. S1 Frontier molecular orbital distribution of studied molecules.

S2. Crystal structure prediction

Currently, our studied molecules have been synthesized in the experiment except for anti-β-MS-NDT and anti-β-MS-ADT. Therefore, we use the USPEX program based on evolutionary algorithm to make the crystal structure prediction for anti-β-

MS-NDT and anti-β-MS-ADT. In whole prediction process, seven space groups with the serial numbers of 2 ($P\bar{1}$), 4 ($P2_1$), 14 ($P2_1/c$), 15 (C2/c), 19 ($P2_12_12_1$), 33 ($Pna2_1$), 61 (Pbca) were selected for prediction, which has been confirmed that more than 80% of the organic semiconductor crystals have the symmetric properties shown by these seven space groups. The initial structures are randomly generated from the above seven space groups, while the structures of the next generation are generated from the structures of the previous generation through genetic and mutation algorithm calculation, and then more than 1000 structures are finally obtained through continuous search and optimization. The optimization process mentioned above is carried out in VASP installation package with PBE functional at 1 atm atmospheric pressure and room temperature, and output the results including enthalpy, density and other cell parameters. Finally, the predicted structures with the lowest enthalpy of formation are taken as the final crystal structures. Using the above method, we first predicted the anti-β-MT-BDT and anti-β-MS-BDT crystals that had been synthesized experimentally in the system to ensure the reliability of the method, and the results placed in **Table S1.** According to the data in **Table S1**, the overall volume error is 2.46% for anti-β-MT-BDT and 1.33% for anti-β-MS-BDT, such a small error range ensures the reliability of crystals predicted by the software. Furthermore, the **Table S2** shows cell parameters of the predicted two crystals.

Table S1 The cell parameters of anti-β-MT-BDT and anti-β-MS-BDT crystals predicted in USPEX and the experimental data

Molecules	anti-β-MT-BDT (Exp)	anti-β-MS-BDT (Exp)	anti-β-MT-BDT (USPEX)	anti-β-MS-BDT (USPEX)
Space Group	$P2_1/c$	$P\bar{1}$	$P2_1/c$	$P\bar{1}$
a(Å)	8.373	5.320	8.483	5.179
b(Å)	13.973	7.289	13.781	7.930
c(Å)	5.341	8.319	5.237	8.269
α(°)	90.000	81.060	90.000	113.142
β(°)	99.362	80.925	79.231	97.042
γ(°)	90.000	71.704	90.000	102.559
V($Å^3$)	616.559	300.530	601.401	296.525

Table S2 The cell parameters of anti-β-MS-NDT and anti-β-MS-ADT crystals predicted theoretically

Molecules	anti-β-MS-NDT	anti-β-MS-ADT
Space Group	$P\bar{1}$	$P\bar{1}$
a(Å)	7.624	7.196
b(Å)	9.838	7.281
c(Å)	5.096	8.867

α(°)	85.752	73.903
β(°)	89.991	66.713
γ(°)	69.016	90.294

S3. Intermolecular stacking modes and weak intermolecular interaction

Table S3 The symbols "B-N" and "B-A" represent the dimer at the same position as in Table3 when X=N and A in the skeleton, the following data are SAPT decomposition energies of them (kcal mol^{-1})

Molecules	Dimer	E_{elec}	E_{exch}	E_{ind}	E_{disp}	$E_{SCS\text{-}SAPT0}$
B-N	mol1-mol2	-4.97	10.15	-3.07	-15.59	-13.47
		14.72%	30.06%	9.09%	46.14%	
C-N	mol1-mol3	-1.76	2.01	-0.25	-2.56	-2.57
		26.75%	30.55%	3.80%	38.91%	
B_1-N	mol1-mol2	-103.53	249.93	-20.23	-58.31	67.86
		23.97%	57.85%	4.68%	13.50%	
C_1-N	mol1-mol3	-19.06	48.06	-6.55	-14.66	7.79
		21.58%	54.41%	7.42%	16.59%	
B_2-N	mol1-mol2	-153.22	337.66	-30.02	-68.73	85.69
		25.99%	57.27%	5.09%	11.66%	

C_2-N	mol1-mol3	-21.62	54.98	-7.34	-16.38	9.64
		21.55%	54.80%	7.31%	16.33%	
D_1-N	mol1-mol2	-10.58	21.11	-2.32	-30.83	-22.61
		16.32%	32.56%	3.58%	47.55%	
E_1-N	mol1-mol3	-2.33	5.65	-0.99	-7.23	-4.90
		14.37%	34.88%	6.11%	44.65%	
D_2-N	mol1-mol2	-15.99	34.26	-3.80	-39.64	-25.17
		17.07%	36.57%	4.06%	42.31%	
E_2-N	mol1-mol3	-5.35	7.67	-1.37	-9.26	-8.31
		22.64%	32.43%	5.79%	39.14%	
B-A	mol1-mol2	-5.64	11.17	-1.68	-18.89	-15.04
		15.09%	29.88%	4.49%	50.54%	
C-A	mol1-mol3	-2.76	3.97	-0.53	-3.51	-2.83
		25.67%	36.85%	4.88%	32.60%	
B_1-A	mol1-mol2	-114.33	276.89	-21.40	-67.09	74.08
		23.83%	57.72%	4.46%	13.98%	
C_1-A	mol1-mol3	-16.02	38.45	-5.55	-12.79	4.10
		22.00%	52.81%	7.62%	17.56%	
B_2-A	mol1-mol2	-171.33	380.89	-31.72	-78.97	98.88
		25.85%	57.46%	4.79%	11.91%	
C_2-A	mol1-mol3	-17.74	42.95	-6.23	-13.92	5.06
		21.95%	53.13%	7.70%	17.22%	
D_1-A	mol1-mol2	-10.47	22.33	-2.56	-32.17	-22.87
		15.51%	33.06%	3.80%	47.63%	

E_1-A	mol1-mol3	-2.95	6.64	-1.14	-9.64	-7.08
		14.46%	32.62%	5.58%	47.34%	
D_2-A	mol1-mol2	-12.69	28.88	-2.83	-31.43	-18.07
		16.73%	38.09%	3.73%	41.45%	
E_2-A	mol1-mol3	-9.33	19.77	-2.16	-24.56	-16.28
		16.71%	35.42%	3.87%	44.01%	

Table S3 (continued)

S4. Calculation details about thermal disorder

We used the Force module in the Material Studio package to complete the molecular dynamics simulation based on the molecular supercell. Wherein, the supercellular size is 4*3*4 for anti-BDT and anti-NDT, 3*3*3 for anti-ADT, 2*2*5 for anti-β-MT-BDT, 2*2*4 for anti-β-MT-NDT, 3*2*4 for anti-β-MT-ADT, 9*3*9 for anti-β-MS-BDT, 9*9*9 for anti-β-MS-NDT and 3*4*10 for anti-β-MS-ADT, separately. The parameters of dynamic simulation were set as NVT ensemble, Berendsen temperature coupling method, Dreiding force field, 300K temperature, 150ps total simulation time and 1fs time step. The structures would be extracted from the simulated trajectory when the whole molecular dynamic simulation reached the thermal equilibrium, and then the transfer integral of the extracted structures were calculated in ADF package at the PW91/TZP level.

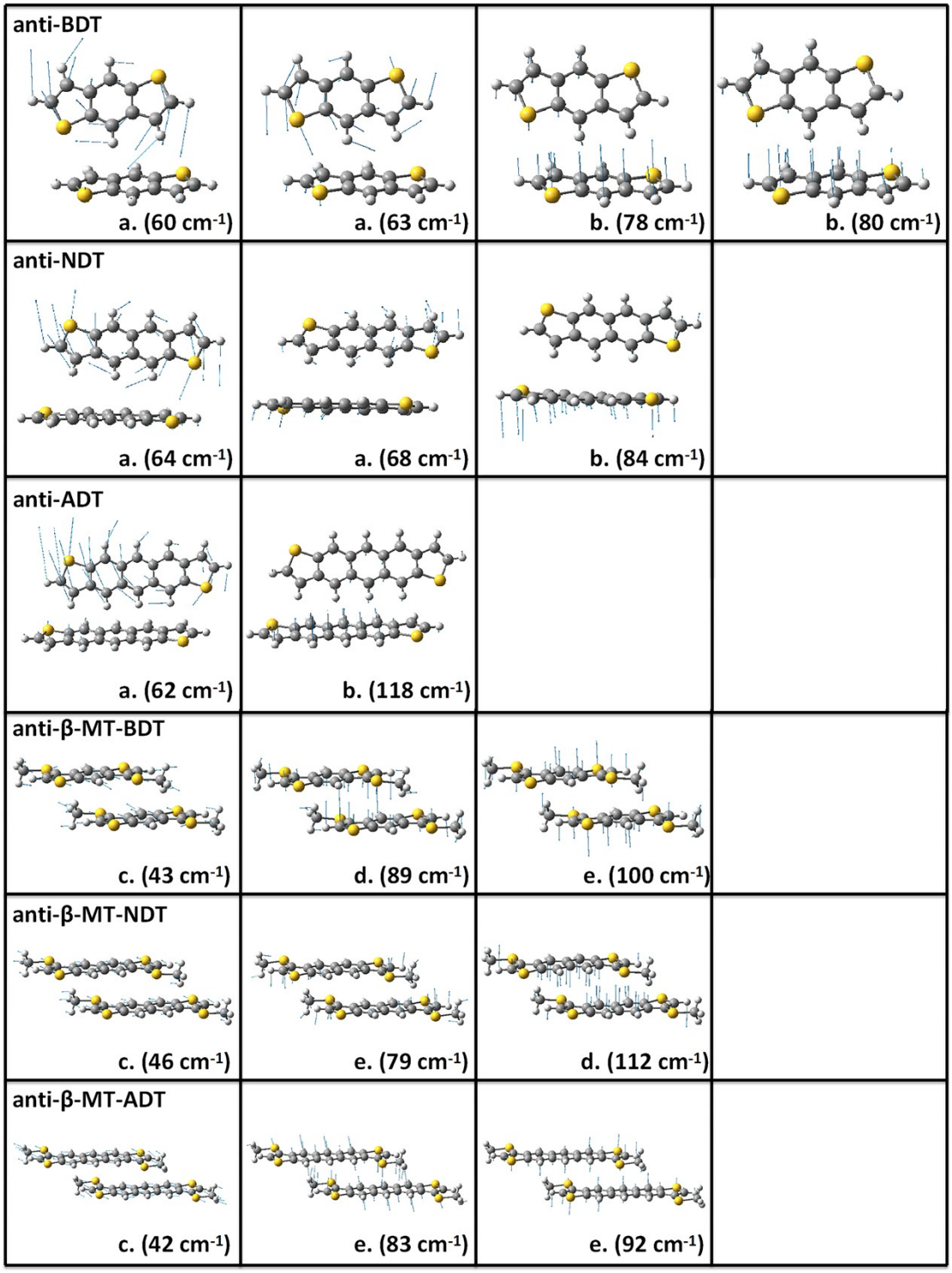

Fig. S2 The intermolecular phonon vibration mode of the system molecules

anti-β-MS-BDT 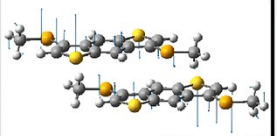 e. (90 cm^{-1})	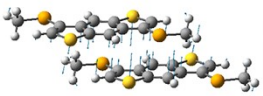 d. (101 cm^{-1})		
anti-β-MS-NDT 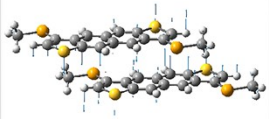 e. (73 cm^{-1})	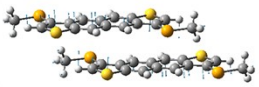 e. (99 cm^{-1})		
anti-β-MS-ADT 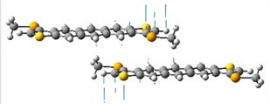 e. (94 cm^{-1})	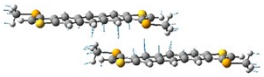 d. (119 cm^{-1})		

Fig. S2 (continued)

References

1. D. K. Hwang, R. R. Dasari, M. Fenoll, V. Alain-Rizzo, A. Dindar, J. W. Shim, N. Deb, C. Fuentes-Hernandez, S. Barlow, D. G. Bucknall, P. Audebert, S. R. Marder and B. Kippelen, *Advanced Materials*, 2012, **24**, 4445-4450.

2. Y.-C. Chang, M.-Y. Kuo, C.-P. Chen, H.-F. Lu and I. Chao, *The Journal of Physical Chemistry C*, 2010, **114**, 11595-11601.